

Misc
reprints

H. Tracy Hall
RES. LAB. REPRINT 3421

GENERAL  ELECTRIC
Research Laboratory

FLAT PANEL VACUUM THERMAL INSULATION

BY

H. M. STRONG, F. P. BUNDY, and H. P. BOVENKERK

SCHENECTADY, NEW YORK

Flat Panel Vacuum Thermal Insulation

H. M. STRONG, F. P. BUNDY, AND H. P. BOVENKERK
General Electric Research Laboratory, Schenectady, New York

(Received June 8, 1959)

Evacuated mats of glass fiber made up of fibers of proper size and orientation are capable of supporting a compressive mechanical loading of at least one atmosphere and yet maintain a thermal conductivity of less than 10 microcalories/cm²°C sec. The use of such a glass fiber mat as a filler makes possible an evacuated flat-panel thermal insulation which is comparable to a Dewar flask in insulation efficiency. The rate of heat transfer through a Dewar flask wall was reduced several-fold at liquid nitrogen temperatures and below by adding a 2-cm-thick layer of orientated and evacuated glass fiber mat to the outer surface.

This investigation showed that in evacuated glass fiber mats, supporting external atmospheric loading, the fiber to fiber contact area is less than 10⁻⁴ the mat area, making the contact pressure about 15 000 kg/cm². The effective length of the thermal conduction paths along the fibers is about four times the mat thickness. The mean pore size for gas molecule motion in the mat was found to be about 54×10⁻⁴ cm and 2×10⁻⁴ cm for mean fiber sizes of 14×10⁻⁴ cm and 0.2×10⁻⁴ cm, respectively. The radiation mean free paths for the same fiber sizes were found to be 150×10⁻⁴ cm and 52×10⁻⁴ cm, respectively. The thermal diffusivity is about 10⁻⁴ cm²/sec, which is much smaller than any other insulating material.

I. INTRODUCTION

ONE of the most effective types of thermal insulation known is a wall space evacuated to less than one micron pressure and having surfaces highly reflective to thermal radiation. In the form of the familiar Dewar flask, this type of insulation has been in use for over sixty years. However Dewar-type insulation is limited to cylindrical and spherical shaped vessels because of the necessity of supporting the atmospheric load by the inner and outer walls without any mechanical support in the evacuated space between. No insulation has appeared in flat panel form that approaches the vacuum type wall in insulation efficiency. Almost all of the other familiar insulations contain air, and regardless of their makeup have the conductivity of still air as their lower limit of conductivity. Few of them reach this lower limit and only the finest particle insulations such as the silica aero-gel of Kistler¹ have conductivities equivalent to, or slightly lower than that of still air. The lowest thermal conductivities can be reached only by removal of air.

A variation of the highly evacuated empty wall space is the moderately evacuated wall space containing lightly packed powders proposed by Smolukowski,²

Langmuir,^{3a} and Stanley⁴ for cylindrical and spherical containers. While such a heat barrier is roughly equivalent to a Dewar-type wall, attempts to use powders to support flat evacuated walls^{3,5,6} were not as successful because of the high thermal conductivity of the same powders when compacted by the atmospheric pressure load.

The possibility of discovering a supporting structure for flat evacuated walls that has great stress bearing capacity and exceedingly low thermal conductivity is very intriguing. The present report describes the authors' study of this and associated problems.

References of further interest in connection with this subject are text books on the kinetic theory of gases,^{7,8} the early work of Smolukowski⁹ and Knudsen¹⁰ on the application of the kinetic theory of gases to explain

³ Unpublished work of (a) I. Langmuir and (b) A. W. Hull, made available to authors.

⁴ W. Stanley, powder filled vacuum wall flask, U. S. Patent 1,071,817 (1913).

⁵ C. G. Munters, U. S. Patent 2,164,143 (1939).

⁶ Blat, Bresler, and Ryabinin, *J. Tech. Phys. (USSR)* **15**, 916-23 (1945). Yu N. Ryabinin (thesis) from Kislodod (1944), No. 3, pp. 39-43.

⁷ Saul Dushman, *Vacuum Technique* (John Wiley & Sons, Inc., New York, 1949).

⁸ E. H. Kennard, *Kinetic Theory of Gases* (McGraw-Hill Book Company, Inc., New York, 1938).

⁹ M. Von Smolukowski, *Akad. Wiss. Wien* **107**, 304 (1898); **108**, 5 (1899).

¹⁰ M. Knudsen, *Ann. Physik* **34**, 593 (1911).

¹ S. S. Kistler, *Nature* **127**, 741 (1931); *J. Phys. Chem.* **39**, 79-85 (1935).

² M. Von Smolukowski, *Krakauer Anz.*, 129(A) (1910); Max Jakob, *Heat Transfer* (John Wiley & Sons, Inc., New York, 1949), p. 90.

TABLE I. Comparison of approximate thermal conductivities in the temperature range 0° to 100°C.

Substance	Coefficient of thermal conduction, k in microcalories/cm ² °C sec
1. Structural materials	
Metals	100 000
Organic polymers	400
Ceramic and refractory materials	10 000
Glass	3 000
2. Insulations	
Air filled fibers, foams, etc., in common use	80
Still air 65°C	69
Finest powders 65°C (silica aero-gel)	60
Dewar flask (66°C inner T) (65°C outer T)	7 microcalories/cm ² sec
Flat vacuum wall structure (max. value desired)	10

gaseous conduction, Smolukowski's² early experiments on gaseous conduction at reduced pressure in fine powders, papers by Kistler¹ on the properties of his silica aero-gel, tests on evacuated silica aero-gel for liquid air storage by Blat *et al.*,⁶ and studies on mechanisms of conduction in air-filled, evacuated and heavy-gas-filled insulations by Verschoor and Greebler.¹¹

II. PHYSICAL REQUIREMENTS

To be comparable with a Dewar flask in insulation quality, the mechanical supporting structure between the walls of a flat vacuum panel should have an effective thermal conductivity not exceeding 10 microcalories/cm²°C sec.* Thus, the supporting structure must have very small contact areas and devious heat flow paths of high thermal resistance. Small contact areas imply high contact stresses attainable only with hard, strong materials which can maintain their properties under conditions of vacuum bake-out and long service life without creep. It is also desirable that the geometry of the supporting structure provide radiation baffling, and that it divide the space into cells small enough that gaseous thermal conduction would be negligible up to gas pressures of a few hundred microns.

In choosing a material to support flat walls against an atmospheric pressure load it is helpful to compare the approximate thermal conductivities of a variety of substances with the desired conductivity of the supporting structure. The values are noted in Table I.

Most glass, ceramic, and refractory materials are hard stable substances suitable for use in permanently evacu-

¹¹ J. D. Verschoor and P. Greebler, *Trans. Am. Soc. Mech. Engrs.* 74, 961 (1952).

* The unit of thermal conductivity used throughout this report is the microcalorie/cm²°C sec. This unit will not be repeated except where necessary for clarity. Thermal conductivity values given apply for an average temperature of the insulation within the range 0° to 100°C, usually about 70°C. Where there are exceptions or where the exact temperature is important to the discussion, the temperature will be given, otherwise not.

ated containers and are the most favored choice for use in devising a vacuum wall support structure. It is clear from their thermal conductivity values that a suitably low thermal conductivity in these materials must be achieved through proper geometric distribution of the support material. It was found that a pad made of glass fibers oriented randomly in planes parallel to the pad (perpendicular to the temperature gradient) fulfilled all requirements.

The thermal conduction characteristic of a number of granular and fibrous substances taken from the authors' test results are shown in Table II. The tests were all made in a one to 10 micron vacuum with a temperature range across the sample of about 20° to 110° or at an average temperature of 65°C. In some tests the sample supported the load of the atmospheric pressure; in others the atmospheric pressure load was not applied to the sample. From the numbers in the table it is readily seen that granular materials are sensitive to applied pressure while fibrous materials are not.

A glass column structure was proposed by Hull¹² of this laboratory which has a solid thermal conductivity very close to 10. Each column consisted of two $\frac{3}{16}$ -in.-diam glass beads in series, one on top of the other in the direction of heat flow. The columns were positioned three or four inches apart by a plate structure lying perpendicular to the direction of heat flow. In an open structure of this sort the wall surfaces are made reflecting and the air pressure kept below about 1 μ of mercury. To the authors' knowledge, this is the only structure for

TABLE II. Thermal conductivity of granular and fibrous materials in a 1 to 10 μ vacuum; average temperature approximately 65°C.

Material	Thermal conductivity, k , microcalories/cm ² °C sec	
	Loosely packed	1 atm Compressive load
80 mesh foundry sand	8.7	86
Glass beads $\frac{3}{16}$ -in. diam	27	98
Glass beads, 0.002-in. diam		50
Crushed Pyrex glass 20 mesh	7.1	23
Carborundum 150 mesh		220
Alumina 100-250 mesh		196
Diatomaceous earth and carbon black 3:1 mixture		51
Silica aero-gel		22
Duck feathers (eider down)		8.3
Asbestos lint		30
Cotton fibers		19
Stainless steel wool (fine)		26
Glass needles 125 μ diam		39
Glass fibers 14 μ diam (good orientation)	9.6 ^a	6 to 8
Glass fibers 4 μ diam (good orientation)	4 to 5	3.9 to 5.2
Glass fibers 2 μ diam (good orientation)		5.4
Glass fibers 0.2 μ diam (good orientation)		4.6

^a Sample thickness under no load increased without much change in heat transfer, making the loosely packed k larger than the k under a compressive load. (See Sec. VI for description of test methods and definition of k .)

flat wall evacuated insulations other than a glass fiber mat approaching 10 in conductivity.

To account for the exceptionally low thermal conductivity of evacuated glass fiber structures, the mechanism of heat flow by gaseous, solid, and radiative conduction will be examined briefly in the sections that follow.

III. SOLID CONDUCTION IN GLASS FIBER SUPPORTS

An exact analysis of heat conduction along the solid paths in a random arrangement of fibers would be a very difficult task. It would be complicated by the existence of radiant heat transfer through the fibers, and at any point there may be an exchange between solid and radiative heat transfer. However, one can visualize an idealized structure consisting of a symmetrical array of uniform fibers like that shown in Fig. 1(a) in which the general heat flow is perpendicular to the fibers. An analysis of a structure of this sort helps to show how glass fiber mat can have so high a thermal resistance, and indicates approximate values of the areas of contact, contact pressures, and path lengths for heat flow.

At the points of intersection of the fibers there will be a tiny circular contact area whose radius b , is given by the Hertz formula¹²

$$b = 1.13(SR/E)^{1/3},$$

in which S is the load per contact, R is radius of fiber, E is modulus of elasticity. The heat must pass through these tiny contact areas and along the fiber to the next contact as shown in Fig. 1(b). The heat flow is assumed to be evenly divided to the right and left.

Focusing attention on the flow to the right only, the symmetry of the flow lines is closely equivalent to the geometry for flow shown in Fig. 1(c) in which the ends of the fibers are pictured as being hemispherical and in contact end to end. The actual contact area between the two fibers is shared equally by the flow to the right and the flow to the left. Hence, the thermal resistance of one contact unit [Figs. 1(b) and 1(c)] is made up of the hemispherical end, with contact area one-half the actual contact area, and a length of fiber, l , equal to one-half the distance between successive fiber junctions. Since the heat leaving each contact point has the opportunity of flowing in two directions, the thermal resistance of each layer is that of two parallel paths, each path consisting of two contact units in series.

In Fig. 1(b), the area of contact due to the pressure flattening is given by the expression

$$\frac{1}{2}\pi b^2 = (\pi/2)1.28(SR/E)^{2/3}. \quad (1)$$

This corresponds to a compression of the radius of the equivalent hemispherical end [see Fig. 1(c)] of an

¹² See S. Timoshenko, *Strength of Materials* (D. Van Nostrand Company, Inc., New York, 1945), Part II, Chap. VII.

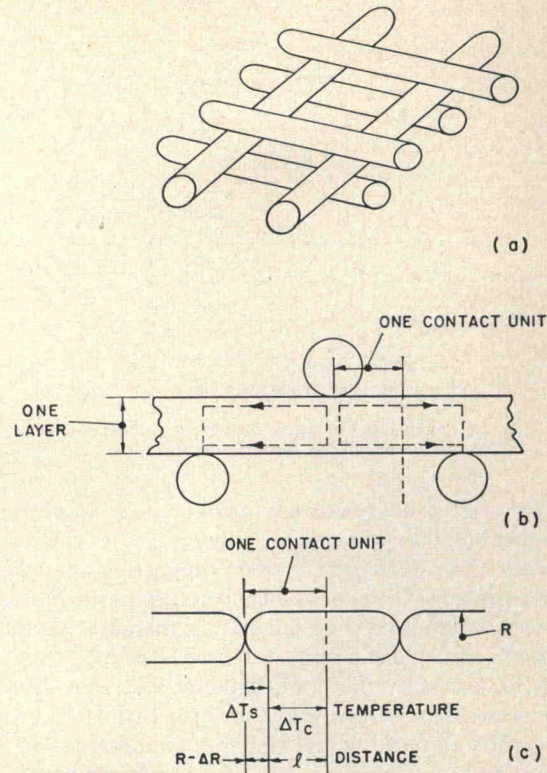


FIG. 1. Ideal glass fiber lattice. (a) A symmetrical lattice of glass fibers; (b) detail of a series of two fiber junctions showing the heat flow path; (c) an idealized fiber junction which is approximately equivalent thermally to the junction shown in (b).

amount given by

$$\begin{aligned} \Delta R &= (\text{area of contact}/2\pi R), \\ &= (1.28/4)(S/E)^{2/3}R^{-1/3}. \end{aligned} \quad (2)$$

The thermal resistance of one contact unit [Fig. 1(c)] was taken to be the sum of the thermal resistances of the hemispherical end ($\Delta T_s/q$) and the cylindrical portion ($\Delta T_c/q$), where q is the rate of heat flow through the fiber. This was found to be

$$\frac{\Delta T_s + \Delta T_c}{q} = \frac{\Delta T}{q} = \frac{1}{2\pi k R} \ln \frac{4R}{\Delta R} + \frac{l}{\pi k R^2}. \quad (3)$$

The first term on the right applies to the hemispherical end and the second term to the cylindrical portion. ΔT is the temperature drop across one contact unit.

The total rate of heat flow, Q , through a one square centimeter area of panel for a temperature difference ΔT across each contact unit will be $2nq$, where n is the number of fiber junctions in one square centimeter and the factor 2 accounts for the two parallel paths of heat flow entering and leaving each fiber junction. From Eq. (3), the value of Q is given by

$$Q = 2nq = \frac{4\pi R^2 k}{R \ln(4R/\Delta R) + 2l} n \Delta T. \quad (4)$$

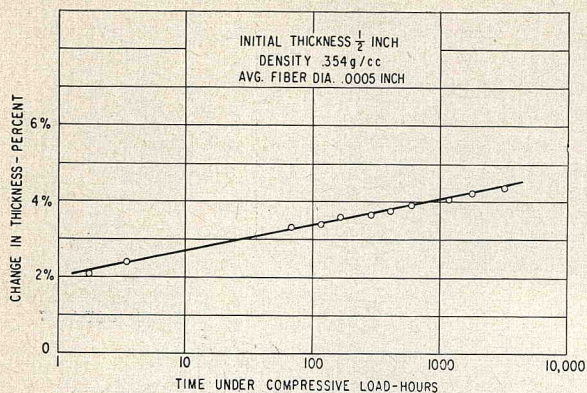


FIG. 2. Decrease in thickness of a glass fiber mat with time under an atmospheric pressure load.

Typical glass fiber mats having fibers with an average diameter of 0.00036 cm and occupying 10% of the space (density about 0.25 g/cm³) when supporting an atmospheric pressure load, had solid conductivities ranging between 4.5 and 5.2. For calculating the effective solid conductivity of such a mat, it must be assumed that all fibers have exactly the same diameter and are laid in a symmetrical lattice array as shown in Fig. 1(a). From the density of packing and the fiber diameter it can be determined that there are 2.78×10^3 layers of fibers in a mat one centimeter thick, and that the fibers in a single layer are spaced four fiber diameters apart so that $l = 4R$. In each layer the fibers are laid parallel with 360 fibers to each centimeter. The number of fiber junctions between layers is therefore $(360)^2$ or 13×10^4 . Each contact in supporting the atmospheric pressure must carry a burden of $10^3/13 \times 10^4$ g or 7.5 d.† The value of ΔR was obtained through the use of Eq. (2). The value of E used was 7×10^{11} d/cm².

Assuming a temperature difference of 1°C across the 1-cm-thick mat, the temperature difference across one contact unit, ΔT , will be 1.8×10^{-4} °C. Substitution of all the data in Eq. (4) gives for Q the value 10 microcalories/sec. Since the conditions chosen for calculating Q were a 1°C temperature difference across a 1-cm cube, this value of Q is also the value for the effective coefficient of solid conduction in microcalories/cm°C sec. The value 10 is to be compared with the values 4.5 to 5.2 obtained experimentally.

Tests on mats of fibers averaging 13×10^{-4} cm in diam gave "solid" conductivity values between 6 and 8 as compared to the theoretical value of 24. Fibers of 125×10^{-4} cm average diameter gave "solid" conductivity values around 18 contrasted to the theoretical value of about 300. The variation between the theoretical and experimental values is in the direction to be expected due to deviation from the perfect lattice assumed. Variation of diameters of the fibers and randomness of orientation in planes causes a smaller

† The area of each contact was about 5×10^{-10} cm² and the pressure about 15 000 kg/cm².

number of contacts than was assumed in the ideal lattice. The greater lateral stiffness of the larger fibers would be expected to enhance this effect still more.

The possibility of fiber breakage and eventual loss of insulating effect over a long period of use has been investigated for 3.6- μ - and 13- μ -diam fibers. Upon first loading the fibers a great many of them can be heard snapping if the ear is placed close to the fibers. The fiber snapping may continue for several hours but with steadily diminishing frequency until it eventually stops. The breakage continues longer for coarse fibers than for fine ones. After the initial adjustment period, the load distribution stabilizes. Evidently the fiber contacts are stressed nearly to their ultimate strengths even in the final stable state.

Measurements of the change in fiber mat thickness as a function of time have been taken and are shown in Fig. 2. Fiber breakage always ceases before any noticeable increase in solid conduction occurs. A number of vacuum insulation panels have been in use for nine years, and have been perfectly stable during this period. Many of them have been subjected to severe mechanical jarring without noticeable change in thickness or insulating value.

IV. GASEOUS CONDUCTION IN POROUS MEDIA

The mechanism of the thermal conductivities of gases was explained by the kinetic theory of gases largely through the efforts of Smolukowski⁹ and Knudsen¹⁰ at the turn of the century. (References 7 and 8 have detailed accounts of this work.) Two different types of gaseous conduction were distinguished, one a pressure independent region of conduction ranging from atmospheric pressure down to fairly low pressures, and the other a pressure dependent region at quite low pressures. The transition from the one type of conduction to the other occurs at pressures where the mean free path for collision between gas molecules is about equal to the mean free path for collisions between gas molecules and the walls of the container, or the particles of the porous structure inside the walled container.

The familiar expression giving the coefficient of thermal conductivity of a still gas, k , is

$$k_{\text{gas}} = A\rho C_v v_a L_g, \quad (5)$$

where ρ is the gas density, C_v the specific heat at constant volume, v_a the average molecular velocity, L_g the mean free path of gas molecules and A a numerical constant. Over a wide range of pressures, k is independent of pressure because L_g varies inversely with the pressure while ρ varies directly with the pressure. When the pressure is reduced below the point where $L_g \sim d$, the distance between the walls or particles against which molecules strike, k becomes proportional to the pressure. At these pressures the mean free path, L , of the molecules, taking into account both collisions between gas molecules and between gas molecules and solid barriers,

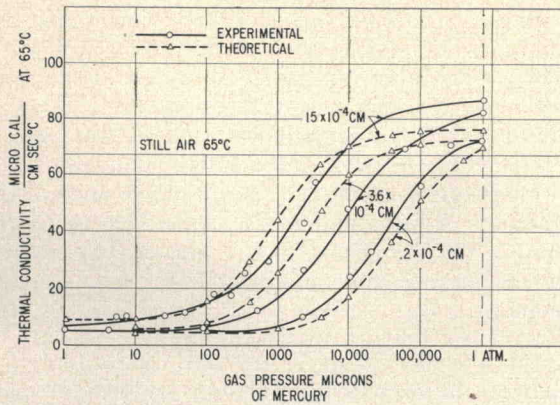


FIG. 3. Thermal conductivity as a function of residual air pressure in insulations of different fiber diameters. Theoretical curves obtained from Eq. (6).

becomes

$$L = L_g [d / (d + L_g)].$$

At pressures such that $L_g \ll d$, $L \approx L_g$. Thus, Eq. (5) taking into account the full range of pressure from atmospheric down may be written

$$k = A \rho C_v v_a [L_g d / (d + L_g)]. \quad (6)$$

In writing Eq. (6), it is assumed that the accommodation coefficient between gas molecules and the particles is unity. If this coefficient is less than unity, the k calculated from Eq. (6) will be too large.

Equation (6) is useful for predicting the gaseous conduction in a porous medium as a function of pressure provided the pore dimension, d , is known. Conversely, it is useful for determining the size of pores in a finely-divided material if one knows how its thermal conductivity varies with the gas pressure. Kistler¹ made use of this relation to determine that the size of the pores in his silica aero-gel was about 5×10^{-6} cm.

For the glass fiber mats used in this work, it was possible to calculate the pore size d in the direction of heat flow and to predict the gas conduction within the mat for various pressures. With the optimum fiber arrangement as described in the previous section, the distance, d , a gas molecule can travel on the average in the direction of heat flow between collisions with glass fibers is given by

$$d = \pi R / 2s,$$

in which R is the fiber diameter and s the fraction of space occupied by fibers. Fibers 14×10^{-4} cm in average diameter and packed to a space factor, s , of about 14% had a d value of 54×10^{-4} cm. Fibers that had an average diameter of 0.2×10^{-4} cm packed to a volume density of 9% had a d value of 2×10^{-4} cm. The predicted and experimental values of the thermal conductivity at different pressures are shown in Fig. 3.

At pressures of 1 to 10 μ of mercury in a glass fiber mat, the gas conduction is negligible and only the re-

sidual solid conduction and radiative heat transfer remain. Together these account for 5 to 9 units of heat transfer. This residual heat conduction must be included with the gas conduction computed for a particular pressure to obtain the estimated total conductivity of the glass fiber mat at that pressure.

It is evident from the calculated and experimental data that a space with glass fiber mats supporting an atmospheric pressure load need not be reduced in pressure below about 100 μ of mercury, depending on fiber size, to obtain negligibly low gas conductivity. This is a distinct advantage because pressures between 10 and 100 μ are rather easy to maintain in a vacuum insulation panel whereas to establish a permanent pressure of 1 μ or less would be more troublesome.

Equation (6) suggests the possibility of finding a material whose d value is so small that the gas conduction k at one atmosphere pressure might be reduced to $\frac{1}{10}$ th its normal value. If this could be done, then there would hardly be need for making a vacuum type insulation in order to achieve greatly increased insulation efficiency. To make $d/d + L_g = \frac{1}{10}$, d must be equal to $L_g/9$. At atmospheric pressure, L_g is about 6×10^{-6} cm. If s is taken to be $\frac{1}{10}$, which experience shows is about as dense as small fibers can be packed, the fiber diameters turn out to be 10^{-7} cm. The smallest fibers made available to us averaged 200×10^{-7} cm in diam.

Probably the finest pore sizes yet produced in thermal insulation are in Kistler's silica aero-gel in which the pore size is estimated to be 50×10^{-7} cm. The thermal conductivity of this material is about 60.

V. HEAT TRANSFER BY RADIATION THROUGH FIBROUS MEDIA

It will be assumed that the insulation is made up of fibers of diameters smaller than the gaps of empty space between fibers. For simplicity it will be assumed that when radiation strikes a fiber a fraction ϵ (absorptivity or emissivity) is absorbed and later re-radiated as thermal radiation characteristic of the temperature of the fiber in which it was absorbed.

The projected sidewise area of the fibers in a volume element of thickness dr and unit area is $2sdr/\pi R$. Hence, the probability of radiation being absorbed while traveling across the element in the dr direction is $2s\epsilon dr/\pi R$, and the probability of its penetrating a distance r is

$$P(r) = \exp(-2s\epsilon r/\pi R). \quad (7)$$

Any preferred orientation of the fibers relative to the axis of the volume element will affect the probability of penetration at different angles θ to the axis. Thus, in general

$$P(r, \theta) = \exp[-2s\epsilon r f(\theta)/\pi R], \quad (8)$$

where $f(\theta)$ is a function characteristic of the fiber orientation.

Now consider a spherical element of an extensive

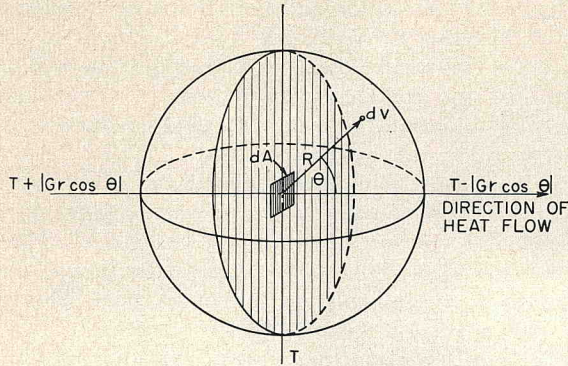


FIG. 4. Radiation through an element of area in an isothermal plane.

uniform volume of insulation which is conducting heat from left to right as shown in Fig. 4. Let the element of area dA at the center of the sphere lie in a plane of equal temperature T . It is assumed that there is a uniform temperature gradient G and that the radiation which passes through the element dA originates and is absorbed within the insulation itself.

The radiation which passes to the right through dA may be obtained by integrating the contributions of all the elements of volume in the half-space to the left. This comes out to be

$$\rightarrow dF_{\text{rad}} = dA \frac{4s\sigma\epsilon}{\pi R} \int_0^{\pi/2} \int_0^{\infty} \sin\theta \cos\theta f(\theta) \times \exp\left[-r \frac{2s\epsilon}{\pi R} f(\theta)\right] [T + |Gr \cos\theta|]^4 dr d\theta. \quad (9)$$

The radiation which passes from right to left is given by a similar expression except that the temperature term is $[T - |Gr \cos\theta|]^4$. The net radiation transfer is the difference of the two integrals. Neglecting some of the small higher order terms this is found to be

$$dF_{\text{rad}} = dA \frac{8\pi R\sigma GT^3}{s\epsilon} \int_0^{\pi/2} \frac{\sin\theta \cos^2\theta}{f(\theta)} d\theta. \quad (10)$$

If the fibers are randomly oriented in all three dimensions $f(\theta) = 1$, and

$$dF_{\text{rad}} = dA (8/3) (\pi R\sigma GT^3/s\epsilon). \quad (11)$$

If the fibers are oriented randomly in planes parallel to dA , then

$$f(\theta) = \cos^2\theta + (2/\pi) \sin^2\theta \quad (12)$$

and

$$dF_{\text{rad}} = dA \cdot 3.24 \cdot (\pi R\sigma GT^3/s\epsilon). \quad (13)$$

If $dA = 1$ and $G = 1$ the expressions given in Eqs. (11) and (13) are just the thermal conductivities by radiation. Thus,

$$k_{\text{rad}} = H \cdot (\pi R\sigma T^3/s\epsilon), \quad (14)$$

in which $H = 2.67$ for complete three dimensional random orientation of the fibers and $H = 3.24$ for the case in which the fibers are randomly oriented in planes perpendicular to the temperature gradient.

Heat transfer by radiation in this case may also be considered as a diffusion of the radiation photons due to a temperature gradient in a space containing a uniform dispersion of radiation baffles. According to general diffusion theory the net flow in the direction of the gradient per unit time and unit of area normal to the gradient is

$$F_{\text{rad}} = (c\lambda/3) (d\rho_{\text{rad}}/dx), \quad (15)$$

where c is the velocity of the photons (velocity of light), λ is the mean free path between absorbing collisions of photons with fibers, and ρ_{rad} is the radiation density. From radiation theory, $\rho_{\text{rad}} = 4\sigma T^4/c$. This, together with Eq. (15), gives the thermal conductivity by radiation in the form,

$$k_{\text{rad}} = (16/3)\lambda\sigma T^3, \quad (16)$$

which is to be compared with the equivalent expression in Eq. (14).

If we equate expressions (14) and (16), using $H = 8/3$, which is the value for three dimensional random orientation of the fibers, a relationship between λ and the fiber pad parameters is obtained:

$$\lambda = \pi R/2\epsilon s. \quad (17)$$

Equation (16) offers the possibility of getting quantitative information about λ from experimental observations. When there is no heat conduction by gases the total heat flow per unit area and time is

$$F = (k_{\text{rad}} + k_{\text{solid}})G = [(16\lambda\sigma T^3/3) + k_{\text{solid}}]G. \quad (18)$$

Remembering that $G = dT/dx$, and integrating, the following relation between temperature and distance is obtained:

$$(4\lambda\sigma/3)T^4 + k_{\text{solid}}T = Fx + \text{const.} \quad (19)$$

Typical graphs of this T vs x relationship are illustrated in Fig. 5. When the heat transfer by radiation is negligible and k_{solid} is independent of the temperature, T vs x is linear. If the heat transfer is by radiation only, the temperature gradient becomes smaller the higher the local temperature, and a nonlinear temperature distribution is established. As both modes of heat transfer occur in actual cases, the observed temperature distribution curves lie between the two extremes just described. If the temperatures are measured at three known positions in a sample conducting heat under steady state conditions of known heat flow rate, three simultaneous equations of the form of Eq. (19) can be written and solved for $4\lambda\sigma/3$, k_{solid} , and the constant of integration. Thus, from such experimental measurements λ and k_{solid} may be determined. Measurements of this type, reported later in this report, gave results which were in fair agreement with the theory.

A more refined theory of transfer of radiation through pads of fiber would have to take detailed account of the reflection of radiation from the fibers, the spectral distribution of the absorptivity of the fiber material, and the effect of the ratio of fiber diameter to wavelength of radiation on the absorption and scattering. Different fiber materials have a considerable range of infrared absorption bands, giving enough difference in total average absorption to show up experimentally (cf. Verschoor and Grebler).¹¹

VI. APPARATUS AND METHODS

The thermal conductivity tests were made by the guarded hot plate method^{13,14} adapted for making tests in vacuum.

A sketch of the apparatus is shown in Fig. 6. The guarded hot plate with a fixed bottom cold plate was enclosed in a steel vacuum chamber. The top cold plate was in the form of a piston which the external atmospheric pressure forced against the test sample to simulate exactly the compression the sample would receive in a vacuum flat panel. A flexible rubber ring diaphragm was used to make the vacuum seal for the piston and still permit free motion of the piston. Several thermocouple connections for measurement and control of temperature were taken through metal-glass seals in the side of the vacuum chamber. Copper tubing was brazed on to the top and bottom plates for circulating cooling water of regulated temperature.

Auxiliary equipment not shown in Fig. 6 included (1) a means for external support of the top plate so that the sample could be tested without any compressive load if desired; (2) stiff springs that could be used for exerting additional force on the piston in excess of the atmospheric pressure; (3) sensitive control equipment

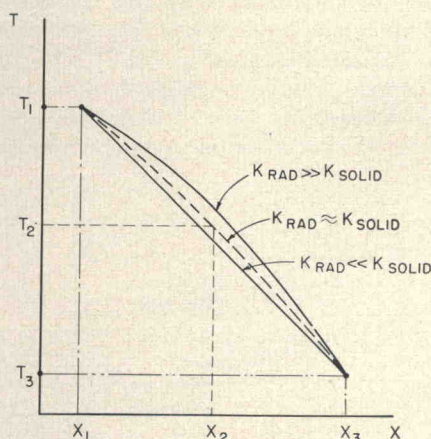


FIG. 5. Temperature vs distance in an evacuated glass fiber mat; x is measured along the thickness of the insulation.

¹³ G. B. Wilkes, *Heat Insulation* (John Wiley & Sons, Inc., New York, 1950), p. 37.

¹⁴ ASTM C-177-45 Standard Thermal Conductivity Test Apparatus; Guarded Hot Plate Method.

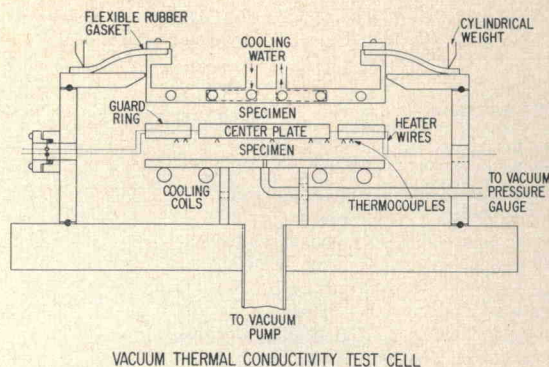


FIG. 6. Apparatus for testing thermal insulation in vacuum under atmospheric pressure load.

to keep the guard ring temperature within 1°C of the center plate temperature; (4) vacuum gauges for measuring pressure inside the sample and other parts of the apparatus; (5) a controlled air leak to enable tests to be made at air pressures ranging from one micron to one atmosphere; and (6) a thin stainless steel collar to rest on the bottom plate for containing granular materials.

The samples tested were usually 1 cm thick and 17.8 cm in diam. Each test was run for sufficient time to be sure that thermal equilibrium was reached. The coefficient of thermal conductivity, k , was calculated from the expression

$$k = (Q \times D) / (A \times \Delta T),$$

in which Q is the amount of power in calories per second to the center plate, D the thickness of sample on one side of the guarded hot plate, A the combined area of both sides of the hot plate, and ΔT the temperature difference between hot plate and cold plate.

VII. TEST RESULTS

A majority of the tests were made with one to ten microns air pressure within the sample, under atmospheric pressure loading and at an average temperature of about 65°C with the cooling water at 20°C and the hot plate at about 110°C . Unless otherwise noted, it will be understood that these were the conditions for the test. A few special tests on radiation effects were made in which either 95°C water or "dry-ice" cooled alcohol was circulated through the coolant tubes.

A number of the characteristics of vacuum types of insulation were studied and the results are given in a series of tables and graphs that follow. First in Table II are listed the thermal conductivities of a variety of substances in vacuum, a few of them in both the loosely packed condition and under atmospheric pressure loading to illustrate the difference in behavior between granular and fibrous types of panel-supporting materials. There are also given results on different glass fiber sizes. Compared to all the other substances tested, including many not given in Table II, properly oriented glass

TABLE III. Influence of coatings on thermal conductivity of glass fiber while supporting atmospheric pressure.

Load material	Coating	k microcalories/ cm ² C sec
Glass fabric woven	Lubricant	79
Glass fabric woven	none	20
PF insulation ^a	Phenolic binder	23
PF insulation ^a	none	10
TWF insulation ^b	Oil coated	18
TWF insulation ^b	none	10
Glass mat ^c	Lubricant	16
Glass mat ^c	none	12
No. 800 Pyrex wool	Small amount lubricant	8
No. 800 Pyrex wool	none	7

^a Owens Corning preformed glass fiber batting.

^b Owens Corning, "thermal wool fiber."

^c Owens Corning glass fiber used for plastic reinforcement.

fiber of 14×10^{-4} cm diam or smaller had by far the lowest thermal conductivity when under a compressive load. In this size range the conductivity was not sensitive to fiber size or compressive load. The 125×10^{-4} cm fibers crumbled almost to a granular powder under the atmospheric pressure load and had a high thermal conductivity compared to the smaller diameter fibers.

The effect of residual air pressure on the thermal conductivities of glass fiber mats was studied by allowing air to leak into the test chamber while throttling the line connecting to the vacuum pump. In this way tests were made at a number of constant pressures ranging from one micron to one atmosphere within the sample. In Fig. 3 are shown the conductivities as a function of air pressure in the sample for glass fiber mats made up of well oriented fibers in three size ranges; 14×10^{-4} , 4×10^{-4} , and 0.2×10^{-4} cm diam. The samples were furnished by the Owens Corning Fiberglas Corporation, Newark, Ohio.

Virtually all glass fiber must have some kind of coating on it to prevent the fibers from "flying" and from

TABLE IV. Influence of fiber orientation on the thermal conductivity of glass fiber^a while supporting atmospheric pressure load.

Material	k microcalories/ cm ² C sec
Glass textile fibers, 6×10^{-4} cm diam laid parallel to each other but perpendicular to direction of heat flow	62
Glass textile fiber randomized in planes perpendicular to heat flow	8
Woven glass fabric 6×10^{-4} cm fibers	20
B fiber, 6×10^{-4} cm fiber arranged mostly parallel to heat flow	72
B fiber random orientation in planes perpendicular to heat flow	3.9 to 5.2
TWF 14×10^{-4} cm fiber diam randomized perpendicular to heat flow. Fibers penetrating several planes	10
HTI fiber improved orientation. Fibers randomized in planes perpendicular to heat flow path. Fiber penetration of adjacent planes reduced	6 to 7

^a All samples supplied by Owens-Corning Fiberglas Corporation.

cutting themselves to pieces. Such coatings cannot be tolerated in a permanently evacuated system since they evolve gases. They also increase the cross-sectional area for heat flow, particularly at the contact points, tending to increase the thermal conductivity of the mat. It is, therefore, essential to remove all coatings by heating before sealing them in a flat vacuum panel.

Tests illustrating the effect of coatings on thermal conductivity are given in Table III. Coatings on the fibers can increase the conductivity two to four times depending on the amount and on the fiber orientation.

Glass fiber may be prepared for use in vacuum panels by first removing the coating by heating, then compressing it to nearly its ultimate density and heating it to a temperature just above the strain point of the glass for a few minutes to permit all the fibers to adapt themselves to a densely packed condition. It is then a coherent and easily handled mat.

The influence of fiber orientation is illustrated in Table IV. The results of tests on fibers are given in which the desired orientation is compared to fibers lined up more or less parallel to each other and with orientations both parallel and perpendicular to the direction of heat flow. Fibers arranged randomly in planes perpendicular to the path of heat flow have the lowest thermal conductivity. Individual fibers should penetrate as few planes as possible in the mat since such penetration tends to short circuit those planes through which the fiber passes.

VIII. EXPERIMENTAL STUDY OF RADIATION TRANSFER

The apparatus was arranged to make temperature measurements at three known positions along the heat flow path in the fiber pads under test. This was accomplished by making some modifications in the sandwich-type thermal conductivity test cell used for the standard thermal conductivity measurements. The modifications are illustrated in Fig. 7. The upper and lower fiber pad samples were each divided into two layers. Each layer was weighed to provide information on the layer thicknesses while under compressive load.

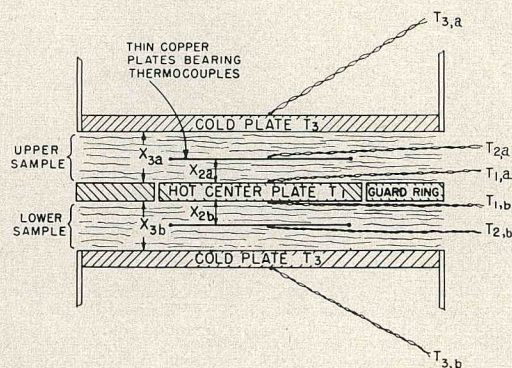


Fig. 7. Experimental setup for analyzing heat transfer by radiation and solid conduction.

TABLE V. Experimental data on heat transfer by radiation in evacuated glass fiber pads.

Fiber designation	Glass "needles"	Glass "thermal wool fiber"	"Glass B" fiber	Glass fiber "filter paper"
Average fiber diameter (cm)	125×10^{-4}	13×10^{-4}	3.6×10^{-4}	0.2×10^{-4}
Fiber orientation	Random	Roughly random in planes	Random in planes	Random in planes
Density (while supporting atmos load) (g cm^{-3})	1.15	0.50	0.25	0.26
s	0.44	0.19	0.096	0.10
λ (cm) [from experiment through Eq. (19)]	0.079	0.015	0.0069	0.0052
$\pi R/2s = \epsilon\lambda$	0.022	0.0054	0.0029	0.00016
ϵ (from $\epsilon\lambda \approx s\lambda$)	0.28	0.36	0.42	0.031
k_{rad} at 10°C	15.0	3.4	1.15	0.85
k_{solid}	18	6.0	4.8	5.0
$k_{\text{rad}}/k_{\text{total}}$ (evacuated insulation)	0.45	0.40	0.20	0.145
$k_{\text{rad}}/k_{\text{total}}$ (air-filled insulation)	0.14	0.04	0.015	0.011

Thin disks of copper, bearing appropriate thermocouples, were placed between the layers to give the temperatures T_{2a} and T_{2b} at the distances x_{2a} and x_{2b} in the upper and lower pads, respectively. The temperatures of the hot center plate, T_1 , and the cold plates, T_3 , were measured with the usual thermocouples attached to them. Care was taken to get a uniform distribution of fiber over the area of the samples. The sample thicknesses were determined by direct measurement of the total thickness ($x_{3a} + x_{3b}$), under test conditions and taking the distances x_{2a} , x_{2b} , x_{3a} , and x_{3b} in proportion to the weights of the corresponding pads of fiber.

Table V lists the results obtained from the experimental tests on pads of different kinds of glass fibers. The average fiber diameters of the different samples ranged from 125×10^{-4} cm to 0.2×10^{-4} cm. The diameters of the fibers within a given sample had statistical distributions similar to that shown in Fig. 8 which is that for the "thermal wool fiber," listed in the second column of the table. The mean free paths λ of radiation were obtained by solution of simultaneous equations of the form of Eq. (19). The values of effective emissivity, ϵ , were obtained by insertion of the above value of λ in the relationship $\lambda = \pi R/2\epsilon s$ [Eq. (17)]. The last two rows of the table compare the fraction of heat transfer by radiation in the same glass fiber pads, evacuated and unevacuated. The greater importance of heat transfer by radiation in the evacuated insulations is striking.

The ϵ 's obtained for the glass "needles," "thermal wool fiber," and the "B" fiber, 0.28, 0.36, and 0.42, respectively, are reasonable considering the competing effect of reflection at glancing angles of incidence. The low value of ϵ for the 0.2×10^{-4} cm diam fiber is to be expected because the diameter of this fiber is many times less than the wavelength of the most intense thermal radiation flux under the test conditions. Apparently after the average fiber diameter gets to be less than about half the wavelength of the most intense ambient thermal radiation, the mean free path of the radiation is set more by the amount of glass it has to go through rather than by the number of fibers.

This approximate lack of dependence of the mean free path of radiation on the average diameter of the fibers for diameters below about 4×10^{-4} cm may also be partially explained by the difference in distribution of numbers of fibers νs fiber mass per unit length as compared to the distribution of numbers of fibers νs fiber diameter. The greater portion of the mass of the glass is concentrated in the fibers of larger diameters, and, hence, the fiber population density is not so high as would be indicated by the gross density, space factor, and "mean fiber diameter." This explanation is strengthened by the observation that the mean free paths of gas molecules in pads of this same nominal 0.2×10^{-4} cm diam fiber, as indicated by experimental measurements, are higher than expected theoretically.

After the values of λ and k_{solid} are experimentally established for a given type of fiber pad, the thermal conductivity characteristics over a wide range of temperatures can be calculated. Figure 9 shows graphically the variation of the thermal conductivities of "TWF" fiber pads and "B" fiber pads with mean temperature using the values of λ and k_{solid} given in Table V. For comparison, experimental points are shown on the same graph. The agreement of the calculated and observed values indicates that the correct mechanism of heat transfer by radiation has been assumed. These data also show the greater radiation baffling effect of the finer

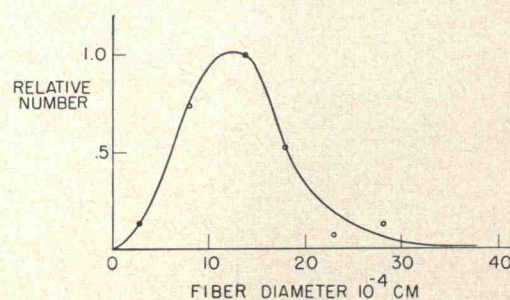


FIG. 8. Distribution of fiber sizes in a sample of thermal wool fiber.

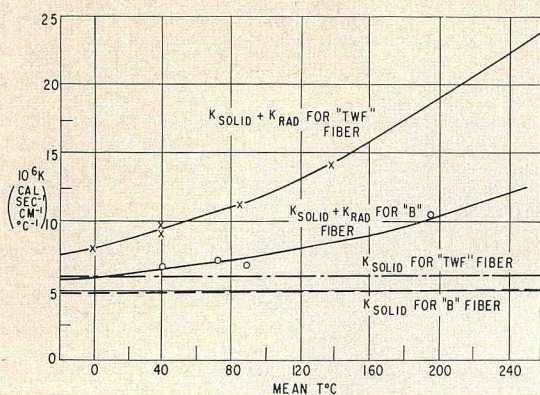


FIG. 9. Thermal conductivity of two types of fiber pads as a function of temperature.

"B" fiber although its gross density is less than that of the TWF fiber.

IX. THERMAL DIFFUSIVITY EFFECTS

The rate at which a wave of temperature change propagates through a medium is determined largely by the thermal diffusivity, $\alpha = k/c\rho$, of the medium, where c is the specific heat and ρ the density. The relatively high heat capacity and unusually low thermal conductivity of the evacuated fiber pad insulations described in this report cause them to have values of thermal diffusivity which are an order of magnitude or more smaller than those of conventional insulations, as shown in Table VI. Preliminary calculations indicated that time intervals of the order of minutes would be required for a temperature shock to penetrate one centimeter of the evacuated insulation. This appeared interesting enough to justify some quantitative tests of this phenomenon.

When a semi-infinite piece of homogeneous conducting medium, bounded by a plane face, and initially at a uniform temperature T_0 throughout (see Fig. 10), suddenly has its face temperature changed to T_1 and held at that value, a plane wave of temperature change propagates through the medium in a direction perpen-

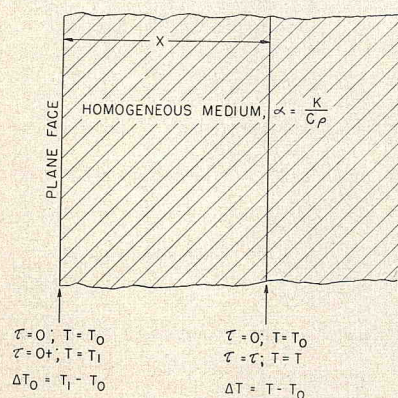


FIG. 10. Thermal diffusion in a homogeneous medium.

dicular to the face. Let this be taken as the x direction. In this simple case the solution of the heat flow equations¹⁵ yields the following relationship:

$$\frac{T_1 - T}{T_1 - T_0} = \frac{2}{\sqrt{\pi}} \int_0^\beta \exp(-\beta^2) d\beta = f(\beta), \quad (20)$$

in which $\beta = x/2(\alpha\tau)^{1/2}$, x is the distance from the face, α the thermal diffusivity, τ the time interval measured from the application of the temperature shock, and T the temperature at a given x and τ . A more convenient arrangement of the relationship is

$$\Delta T / \Delta T_0 = 1 - f(\beta), \quad (21)$$

where ΔT_0 is the temperature change imposed at the face and ΔT is the change from the initial temperature at depth x and time τ .

A convenient way to solve Eq. (21) for a certain ΔT_0 is to take a given value of ΔT and find, by use of tables

TABLE VI. Values of thermal constants for various materials (20°C).

Material	k cal cm ⁻¹ sec ⁻¹ °C ⁻¹	c cal g ⁻¹ °C ⁻¹	ρ g cm ⁻³	α cm ² sec ⁻¹
Silver	0.974	0.0558	10.5	1.66
Aluminum	0.504	0.214	2.70	0.872
Steel	0.115	0.115	7.90	0.127
Marble	0.008	0.203	2.71	0.0145
Glass	0.0028	0.20	2.6	0.0054
Cork	0.00011	0.40	0.14	0.0020
Refrigerator glass fiber	0.000086	0.20	0.032	0.013
Evacuated glass fiber pad	0.0000060	0.20	0.25	0.00012
to	0.0000080		0.40	0.00010

of the $f(\beta)$ function, the value of β which satisfies the equation. From this β and a given x the τ is obtained at which the ΔT occurs. In the experimental tests ΔT_0 was about 97°C, x was nearly 1 cm and α for the insulation was approximately 10⁻⁴ cm² sec⁻¹. The theoretical ΔT (°C) vs τ (sec) curve for this case is shown in Fig. 11. Note that there is practically no change in temperature during the first 360 sec, or 6 min.

The experimental results are also shown in Fig. 11. The observed transit time of the thermal shock was closely that predicted by the theory, but the rate of temperature change from that time on was less than indicated by the theory because of the presence of the metal envelope of the insulation panel. The envelope had considerable heat capacity and much greater thermal conductivity than the filler and so decreased the rate of temperature change. This latter effect was verified by running some tests on an electric analog of the thermal system. The results of the analog computer are also shown in Fig. 11.

¹⁵ Ingersoll, Zobel, and Ingersoll, *Heat Conduction*, McGraw-Hill Book Company, Inc., New York, 1948), Chap. 7.

X. MECHANICAL PROPERTIES OF EVACUATED PANELS

The pressure of the atmosphere holding the envelope of an evacuated panel firmly against the filler pad prevents the envelope from buckling easily and thus develops the "skin-strength" of the structure. For this reason evacuated panels having thin metal envelopes have unusual bending and torsional stiffness.

Although the envelope supplies most of the strength, the fibrous filler pad also contributes because of the fibers being locked together into a board-like structure by the compression. This is readily demonstrated by placing a pad of fibrous filler material in a flexible rubber envelope, sealing it off, and evacuating. Before evacuation the assembly is quite limp and flexible while after evacuation it has about the stiffness and strength of loosely bonded fiber board.

Evacuated panels of glass fiber do not have the acoustic absorbing power of similar pads of air-filled insula-

TABLE VII Heat conduction in Dewar flask walls (5-liter Dewars)

	Standard Dewar No. 1	Standard Dewar No. 2	"Super-Dewar" (2 cm thick glass fiber layer)
Liquid nitrogen evaporation rate			
liter/day	0.691	0.672	0.341
cal/sec	0.306	0.297	0.1515
cal/cm ² sec	1.91 × 10 ⁻⁴	1.86 × 10 ⁻⁴	0.810 × 10 ⁻⁴
Liquid hydrogen evaporation rate			
liter/day		3.00	0.725
cal/sec		0.263	0.0633
cal/cm ² sec		1.64 × 10 ⁻⁴	0.339 × 10 ⁻⁴
Liquid He evaporation rate			
liters/day		22.5	1.75
cal/sec		0.196	0.0153
cal/cm ² sec		1.23 × 10 ⁻⁴	0.082 × 10 ⁻⁴

tion. There are two reasons for this: first, there can be no friction damping of the air motion of sound waves relative to the fibers because the fibers are in a vacuum; and second, the points of contact of the fibers are loaded so heavily by the pressure of the atmosphere that they react elastically rather than dissipatively to vibrations imposed upon the walls of the panel. The acoustic effect is pronounced enough that it is easy to distinguish between identical evacuated and unevacuated panels merely by thumping them.

XI. IMPROVED DEWAR TYPE VACUUM WALL FLASK

Remarkably low heat transfer values can be obtained using a combination of a Dewar flask type radiation gap and an evacuated glass fiber layer. This structure for a five liter flask is illustrated in Fig. 12 and is called a

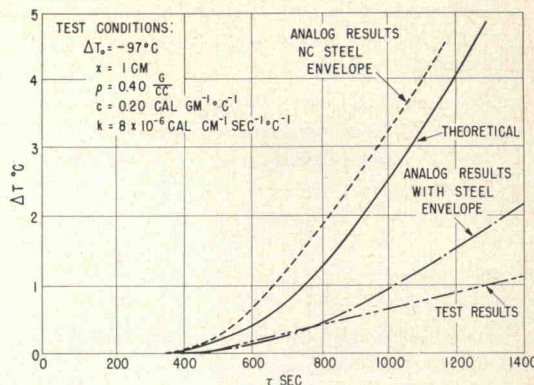


FIG. 11. Temperature vs time on one side of a vacuum panel after applying a thermal shock to the other side.

"super-Dewar" flask.¹⁶ The structure shown was designed for the storage of liquefied gases.

The gain in insulation efficiency over a standard Dewar increased with reduction of the internal temperature. For example, in comparing a five liter "super-Dewar" flask with a standard Dewar of like capacity by measuring the times required to evaporate five liters of a liquefied gas, it was found that liquefied nitrogen lingered two or three times longer in the "super-Dewar" than in the standard Dewar, hydrogen, four times longer, and helium over ten times longer.

It is important for the glass fiber layer to be on the high temperature side of the insulation because its function is to keep the temperature of the warmer side of the radiation gap as low as possible. Then the transfer of heat across the radiation gap is substantially reduced since total radiation across the gap is governed by the difference in the fourth powers of the two temperatures.

The comparative data for liquefied gas storage on the two types of flasks is given in Table VII. The two flasks used were identical standard Dewars initially. Both of them were tested on liquid nitrogen storage first then standard Dewar number one was modified by surrounding it with a two cm thick layer of evacuated "B" fiber glass to convert it to a super-Dewar. The glass fiber mat had properly oriented fibers as previously described and

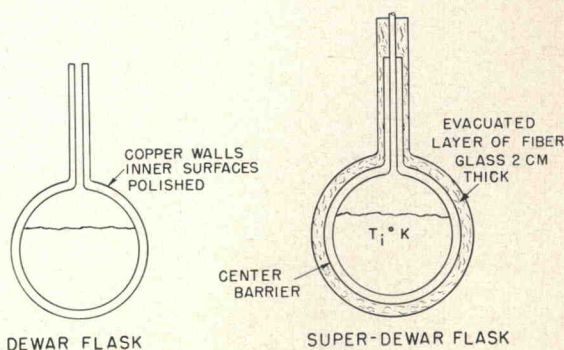


FIG. 12. Standard and super-Dewar structures.

¹⁶ H. M. Strong and F. P. Bundy, US Patent 2,776,776.

its density was about 7 lb per cu ft. The reflecting surfaces of the three Dewars were polished copper. The data in Table VII clearly show the marked improvement in insulating effect due to the glass fiber layer.

In the absence of a temperature measurement on the middle wall, it is not possible to explain this remarkably low heat transfer rate in detail. But it is probable that the conductivity of the glass fiber layer near the inside surface was much reduced, possibly by as much as a factor of ten, at the liquefied gas temperatures over that measured at $\sim 70^{\circ}\text{C}$.

Various modifications of this structure would be likely to show similar effects. For example, multiple radiation gaps or a powder filled outer space might be used. But the glass fiber mat offers structural simplicity because small compact pads of it may be used in direct contact with the inner vessel to support it mechanically without loss of insulation.

XII. CONCLUSIONS

In evacuated, flat, thermal insulating panels, the conduction of the internal structure required to support the walls against the crushing load of atmospheric pressure proved to be the most critical factor. Grits, powders, grills and various kinds of cellular structures all develop unacceptably high conductivities when under compressive loading of the atmosphere. Pads made of fine glass (or glass-like) fibers oriented randomly in planes perpendicular to the temperature gradient and pressure axis proved to have remarkably low thermal conductivity which was quite insensitive to loading. Glass fiber pads

of this type, enclosed in flat metal envelopes gave thermal conductivities in the range of 4 to 10 micro-calories/cm $^{\circ}\text{C}$ sec.

Several other properties of a glass fiber supporting structure are of considerable significance. The radiation baffling of a 1-cm-thick layer is equivalent to that of several highly reflecting surfaces. The pore space between fibers is small enough that internal gas pressures up to about 100 μ may be tolerated without significant impairment of insulating qualities. The thermal diffusivity of this type insulation is at least an order of magnitude lower than for common insulations due to the remarkably low thermal conductivity but relatively high capacity of the glass fiber mat.

Remarkably low heat transfer rates were obtained in Dewar flasks while storing liquefied gases by surrounding the flasks with an evacuated glass fiber blanket.

The stability, permanence of vacuum and high insulating efficiency of the glass fiber structure sealed in evacuated metal envelopes¹⁷ has been well established over a period of nine years of use.

ACKNOWLEDGMENTS

The authors are grateful to A. W. Hull, the late I. Langmuir, M. Hebb, and A. J. Nerad for valuable discussions, and to the Owens-Corning Fiberglas Corporation for supplying samples of especially prepared glass fiber mats.

¹⁷ H. M. Strong and F. P. Bundy, British Patent 715,174 and Canadian Patent 537,151.

GENERAL  ELECTRIC
Research Laboratory
SCHENECTADY, N. Y.